Atomic total electron-capture cross sections from C-, O-, F-, and S-bearing molecular gases for ~MeV/u H^+ and He^+ projectiles

S. L. Varghese
East Carolina University, Greenville, North Carolina 27834
and University of South Alabama, Mobile, Alabama 36688

G. Bissinger, J. M. Joyce, and R. Laubert*
East Carolina University, Greenville, North Carolina 27834

(Received 23 July 1984; revised manuscript received 26 December 1984)

Total single-electron-capture cross sections for H^+ from hydrocarbons [CH_4, C_2H_2, C_2H_4, C_2H_6, $(CH_2)_3$, C_3H_6, C_3H_8, C_4H_8] and the oxide (CO, CO_2, O_2) and fluoride (CF_4, C_2F_6, C_4F_8, SF_6) gases, as well as Ne, have been measured in the projectile energy range 0.8—3.0 MeV. For comparison at 0.8 MeV/u, electron-capture cross-section measurements for 3.2-MeV He^+ were also made on most of these same gases. These systematic measurements display additivity failure in each C_mX_n molecular species. A simple geometrical model, used to estimate intramolecular electron-loss probabilities, allowed extraction of "atomic" σ_{10} values for C, O, F, and S at each projectile energy. These extracted cross sections generally agreed well with total bound-state electron-capture calculations, corrected for the projectile's energy loss and Coulomb deflection, target electron-shell binding and polarization, and relativistic effects.

I. INTRODUCTION

Experimental studies of charge-exchange cross sections date back to as early as 1922 when Henderson[1] used α particles to study the phenomena. Electron-capture cross-section measurements for protons were pursued by Bartels[2] in 1930. Some of the earliest theoretical studies were those by Oppenheimer[3] and Brinkman and Kramers.[4] Since these early ventures many investigations have been made in the area of charge exchange due to the fact that these cross sections are important in design of radiation detectors, astrophysics studies, and in controlled thermonuclear fusion—to mention a few applications. Electron-capture cross-section measurements with bare heavy ions have been made by Shiebel *et al.*[5] whereas Cocke *et al.*[6] extended these cross-section measurements with other heavy ions. A theoretical review of various approaches has been given by Mapleton[7] and very recently by Taulbjerg.[8]

There have been three review papers written regarding the charge exchange of protons and hydrogen, viz., those by Allison,[9] Betz,[10] and Tawara and Russek.[11] Experimental investigations of the total electron-capture cross sections have been made by Welsh *et al.*,[12] Schryber,[13] Toburen, Nakai, and Langley,[14] and Varghese *et al.*[15] *K*-shell differential cross-section measurements have been initiated by Cocke *et al.*[16] and continued by Horsdal-Pedersen, Folkmann, and Pedersen[17] among others. Of these several references regarding previous experimental work on electron capture by protons, that of Ref. 14 must be singled out since it also covered many of the hydrocarbon molecular targets used here, provided a check on our earlier measurements,[15] and supplied electron-capture (and -loss) cross sections used in the extraction of "atomic" capture cross sections.

The theoretical calculations of Mapleton,[18] Bates and Mapleton,[19] and Nikolaev[20] have been the mainstay for comparison of experimental work with theory. Theoretical works of Band[21] and Omidvar[22] have special relevance to the differential cross-section measurements. Another recent theoretical work with references is that of Fritsch and Lin.[23] More pertinent to the present work, however, is the electron-capture theory of Lapicki and Losonsky[24] and Lapicki and McDaniel[25] which provides predictions of the absolute electron-capture cross sections without any scaling. It corrects for the projectile's energy loss (E) and Coulomb deflection (C), perturbed-stationary-state (PSS) effects on target electron-shell binding and polarization, and relativistic (R) effects in the charge-changing collision (hereafter labeled as ECPSSR). Agreement between theory and experiment has been, in general, much better for total capture cross sections than for differential cross sections.

In this work we report cross sections for total electron capture by 0.8—3.0-MeV H^+ and 3.2-MeV He^+ from various molecular gases as well as neon. These measurements have considerably smaller relative errors compared to previous work, and allow observation of the small, but significant, deviations from strict atomic additivity. Using a simple model of intramolecular electron loss collisions, atomic total electron-capture cross sections were extracted for C, O, F, and S from hydrocarbon and the oxides and fluorides of C, as well as SF_6. Although the initial motivation for doing these electron-capture studies resulted from observation of "chemical effects" in C *K* x-ray production cross sections,[26] the measured cross sections and the deviations from additivity are far too small to explain the effects reported in Ref. 26. The chemical effects seen in total electron-capture cross sections are be-

lieved to be entirely independent of those implicated in x-ray production and are so treated in what follows.

II. EXPERIMENT

Protons in the energy range 0.8—3.0-MeV and 3.2-MeV singly charged helium ions from the East Carolina University 2-MV tandem Van de Graaff accelerator were used in the experiment. The beams were collimated by adjustable apertures, typically 0.16 cm in diameter and 0.46 m apart, before entering the differentially pumped gas cell. The experimental arrangement was very similar to that reported in Ref. 15, with the addition of a 15-cm diffusion pump mounted directly underneath the gas cell in the target chamber. The entrance slit of the gas cell was of area 4×10^{-4} cm^2 whereas the exit aperture was of area 2×10^{-2} cm^2. The length of the gas cell was 1.91 cm. Downstream from the gas cell an electromagnet was used to separate the ion beam from the neutral-particle beam. A beam-skimming aperture of area 10^{-1} cm^2, placed 3 cm downstream of the exit aperture of the gas target, was used to prevent any aperture-scattered ions from bouncing off beam tube walls into the neutral-particle detector. A surface-barrier detector with a collimated aperture of 1.2 cm, placed 0.76 m from the exit aperture of the gas cell, served as the neutral-particle detector. A movable Faraday cup was used to collect the original beam and also the deflected ion beam after the magnet. Another Faraday cup could be inserted in front of the surface-barrier detector to monitor alignment and to protect the surface-barrier detector from excessive beam exposure. Gas input into the cell (and the corresponding cell pressure as measured by a 0—1-Torr range capacitance manometer) was regulated by a solenoid-actuated gas-flow valve in a feedback-regulated control system. In the experiment a typical pressure of 10 mTorr was used in the cell. The pressure in the beam line during operation was about $\sim1\times10^{-5}$ Torr.

The collected charge from protons or He^+ ions, deflected away from the initial beam direction into the Faraday cup after passage through the gas cell, was used to determine the number of incident ions, I^+. The very small fraction of neutral particles, I^0, formed in the gas cell from electron capture by protons or helium ions, was measured using the surface-barrier detector. A typical ion current used in the experiment was 10—50 pA, amplified with a standard electrometer, and then connected to a current digitizer.

Corrections for neutral particles formed in the beam line were made by bleeding in the target gas (gas off in gas cell) until the beam-line pressure read the same as in normal gas-cell operation. This correction was typically 10%. In order to remain under single-collision (intermolecular) conditions, measurements were made to ensure linearity of I^0 versus gas-cell pressure plots.

The gases used in the experiment were all readily available, high-purity (99% or better) gases. Single-electron capture by singly ionized H and He projectiles, providing neutral exit beams, was measured with the following gas targets: Ne, hydrocarbons [CH_4, $C_2H_{2,4,6}$, $(CH_2)_3$, $C_3H_{6,8}$, C_4H_8 (four gases)], O_2, oxides ($CO_{1,2}$), fluorocarbons (CF_4, C_2F_6, C_4F_8), and SF_6.

III. DATA ANALYSIS AND RESULTS

The total cross section for electron capture by H^+ or He^+ per gas molecule was determined from $\sigma_{10}=I^0/(nl'I^+)$, where n is the number of gas molecules per cm^3 and I' is the length of the gas cell, corrected for gas leakage through the cell apertures[11] via the relation $l'=l+2(r_1+r_2)$, where the $r_{1,2}$ are the exit and entrance aperture radii.

Table I presents the results of the total electron-capture cross section measurements for 0.8—3.0-MeV protons from various gases. Our absolute uncertainties are 6%, obtained from rms values for the current integration (4%), pressure uncertainty (3%), gas-cell length and aperture measurements (3%), and statistical and peak intensity determination uncertainties (2%). Relative measurements have uncertainties of 2%.

We present the measured cross sections for electron capture by 3.2-MeV singly ionized helium ions from various gases in Table I also. As in the case of σ_{10} measurements of protons, the absolute uncertainty for the helium measurements was 6%.

IV. DISCUSSION

Our experimental results are in very good agreement, where there is overlap, with those of previous investigators.[12–14] It would be very desirable to have some way to compare these molecular capture cross-sections to theoretical predictions, which, of course, are almost without exception for atomic targets. In the discussion that follows we present a method to extract such atomic cross sections from molecular cross-section measurements.

A. "Entrance" and "exit" effects in electron capture from molecules

In a recent letter[27] we presented a way of treating electron capture to bound states (ECB) of H^+ from hydrocarbon molecules that would allow extraction of atomic cross sections. Here we summarize this approach and in subsequent sections extend the procedure via a geometric outscattering (GO) model to other molecules. An approximate, first-order theoretical approach corrected the electron-capture cross sections for each atom in the molecule according to changes in the electron's binding energy and orbital population. This was called the entrance effect and, in the case of hydrocarbons, amounted to less than a 2% correction to the calculated atomic theoretical cross sections.

A qualitative understanding of the insensitivity of the hydrocarbon ECB cross sections to the entrance effect comes by noting that our projectile velocities exceeded any orbital electron velocity in the target hydrocarbon molecules. Hence the K shell will be the dominant contributor of captured electrons, and the target's outer shell(s) will suffer little orbital polarization. The details of the chemical bonds in random orientation should be unimportant for such a high-velocity projectile. Also, the projectile na-

TABLE I. Experimental and fitted molecular electron-capture cross sections for 0.8—3.0-MeV H^+ and 3.2-MeV He^+ on various gases. (All cross sections in 10^{-21} cm^2.) Sufficient significant digits are reported to remain within relative errors of ±2%—absolute errors ±6%. All fit cross sections with $a=3.3$—see text for discussion of fitting procedure.

	Projectile energy (MeV)									
	H^+								He^+	
Target gas	0.8		1.5		2.0		3.0		3.2	
	Expt.	Fit	Expt.	Fit	Expt.	Fit	Expt.	Fit	Expt.	Fit
CH_4 (methane)	45	43	7.5	7.5	2.58	2.62	0.51	0.51	156	154
C_2H_2 (acetylene)	82	80	14.2	14.4	5.0	5.0	0.99	0.99	283	289
C_2H_4 (ethylene)					5.1					
C_2H_6 (ethane)	80	80			5.0	5.0				
C_3H_6 (propylene)	114	112	20.9	20.6	7.2	7.3	1.44	1.44	401	396
$(CH_2)_3$ (cyclopropane)					7.2					
C_3H_8 (propane)					7.2					
C_4H_8 (isobutylene)	140	142	26.5	26.6	9.4	9.4	1.90	1.88	496	500
C_4H_8 (1-butene)					9.5					
C_4H_8 (trans-2-butene)					9.3					
C_4H_8 (cis-2-butene)					9.5					
O_2 (oxygen)	97	98	15.2	14.9	5.7	5.8	1.47	1.47	295	296
CO (carbon monoxide)	88	89	14.7	14.6	5.4	5.4	1.26	1.23	285	294
CO_2 (carbon dioxide)	133	129	20.8	21.1	7.9	8.0	1.87	1.91	418	410
Neon	104		10.7		3.52		0.89			
CF_4 (tetrafluoromethane)	270	271	36.7	38.3	13.1	12.9	3.43	3.39	800	890
C_2F_6 (hexafluorethane)	369	375	54	56	18.9	19.2	5.0	5.1	1190	1210
C_4F_8 (octafluorobutene)	439	430	76	72					1450	1340
SF_6 (sulfur hexafluoride)			69		29.4		6.4			

TABLE II. Calculated transmission fraction for 0.8—3.0-MeV H^+ and 3.2-MeV He^+ on C_mH_n, C_mO_n, C_mF_n, and SF_6 molecules ($a=3.3$).

	Projectile energy (MeV)									
	H^+								He^+	
Molecule	0.8		1.5		2.0		3.0		3.2	
Hydrocarbons	C	H	C	H	C	H	C	H	C	H
CH_4	0.910	0.867	0.945	0.910	0.958	0.922	0.970	0.939	0.896	0.857
C_2H_2	0.878	0.854	0.919	0.900	0.930	0.912	0.946	0.930	0.868	0.845
C_2H_6	0.852	0.830	0.907	0.887	0.924	0.902	0.944	0.924		
C_3H_6	0.801	0.803	0.872	0.869	0.892	0.886	0.919	0.912	0.782	0.788
C_4H_8	0.761	0.783	0.846	0.857	0.868	0.875	0.900	0.903	0.740	0.768
Oxides	C	O	C	O	C	O	C	O	C	O
O_2		0.890		0.918		0.927		0.941		0.877
CO	0.879	0.898	0.909	0.930	0.918	0.938	0.934	0.951	0.865	0.892
CO_2	0.767	0.863	0.826	0.906	0.844	0.917	0.873	0.935	0.740	0.852
Fluorocarbons	C	F	C	F	C	F	C	F	C	F
CF_4	0.581	0.775	0.682	0.841	0.715	0.860	0.770	0.891	0.542	0.753
C_2F_6	0.487	0.700	0.622	0.790	0.663	0.816	0.731	0.856	0.438	0.670
C_4F_8	0.345	0.583	0.531	0.710	0.585	0.745	0.673	0.801	0.284	0.543
	S	F	S	F	S	F	S	F		
SF_6			0.673	0.778	0.709	0.802	0.770	0.852		

vigates the molecule in $\Delta t \cong 10^{-17}$ s; hence associated energy uncertainties would be considerably larger than any typical valence-electron binding-energy variation among the molecules. Because the hydrocarbons have very similar numbers of s and p electrons regardless of the bonds (and with similar binding energies), the number of s and p valence electrons per C atom in each hydrocarbon molecule appears to be the same to the projectile. On account of the dominance of K-shell capture, the net result for the total ECB cross section is still close to atomic values for the C atom in hydrocarbon molecules.

The other correction addressed only what happened to the projectile and its bound electron as it traversed the remainder of the molecule. This was called the exit effect and arose from a second *intra*molecular collision that caused the projectile to lose its electron. The magnitude of the exit effect was estimated from the capture-loss rate equation, viz.,

$$\frac{df^0}{dx} = \sigma_{10} f^+ - \sigma_{01} f^0 , \tag{1}$$

where f^+ and f^0 are the bare and neutral charge-state fractions of hydrogen, $f^+ + f^0 = 1$, and σ_{01} is the electron-loss cross section. The solution of Eq. (1) for f^0 is

$$f^0 = \frac{[(\sigma_{10} + \sigma_{01} e^{-(\sigma_{10}+\sigma_{01})}]}{(\sigma_{10}+\sigma_{01})}$$

$$\simeq e^{-\sigma_{01} x} \tag{2}$$

to within 1% for any projectile or projectile energy used in this experiment. To evaluate Eq. (2) it was assumed that the projectile on the average captured an electron halfway through a "linear" molecule and then interacted with, on the average, half the remaining atoms in the molecule. Using experimental σ_{01} values from Ref. 14, it was straightforward to estimate the probability of an electron-loss collision in the molecule. These probabilities closely agreed with the magnitude and trends in our data, essentially without any adjustable parameters.

B. Geometrical model calculation of exit effect

To bypass some of the geometrical assumptions involved in computing the magnitude of the exit effect with the rate-equation solution described above, an alternate approach—a GO model that still employs the basic concept of intramolecular scattering but is applicable to any molecule with any geometry—is presented.[28] In the GO model the loss cross sections for H^0 (which has picked up an electron while passing by an atom in the molecule) appear as a disk of area σ_{01} at some interatomic distance d_{ij}, and hence subtend a solid angle of $\Delta\Omega_{ij}$ from the donor atom. Summing these solid angles over the whole molecule, dividing by 4π sr, and then averaging over all possible donor atoms of a specific atomic species in that molecule, gives the fraction of the sphere screened and thus the probability P of the H^0 undergoing electron loss while exiting the molecule.

The probability of undergoing electron loss, P, was calculated from

$$P = 0.5 \sum_{i,j} [1 - d_{ij}/(d_{ij}^2 + a\sigma_{01}/\pi)^{1/2}] . \tag{3}$$

The cross sections in Eq. (3) are just the σ_{01} values relevant to the choice of projectile, projectile energy, and atom involved in the loss collision. Implicitly it is assumed that the loss cross sections used here for an atom in a molecule are approximately the same as actual atomic values; the adjustable parameter a, included in Eq. (3), compensates for breakdown of this assumption, as well as the neglect of diffraction effects (expected to be small) and, of course, the unrefined nature of the GO model. From P the transmission fraction $T = 1 - P$ is calculated so that the molecular σ_{10} cross section

$$\sigma_{10}(C_m X_n) = T(C;mn) m \sigma_{10}(C) + T(X;mn) n \sigma_{10}(X) \tag{4}$$

can be computed, *if* the atomic σ_{10} values are known. Equation (4) is our modification of the fundamental additivity equation (which has unity value for all transmission fractions) that generates molecular cross sections from atomic cross sections. The T(C or X;mn) terms are the transmission fractions for the case of either the C or the X (H, O, or F) atom being the electron donor in the initial capture collision.

C. Extraction of atomic from molecular electron-capture cross sections

Generally atomic σ_{10} values are unavailable except for noble gases. Therefore an alternate procedure is outlined. From a systematic measurement of molecular σ_{10} cross sections for a number of two-atomic-species molecules, such as $C_m X_n$, it is possible to deduce associated atomic values if T can be calculated. In Eq. (4) there are three "knowns"—m, n, and $\sigma_{10}(C_m X_n)$—and four unknowns—T(C;mn), T(X;mn), σ_{10}(C), and $\sigma_{10}(X)$. Here X is H, O, or F, and previous σ_{01} results are either readily available or atomic values can easily be estimated[14] from systematic trends in σ_{01} as the target molecule is varied. By computing T values for each projectile, for each projectile-energy—target-molecule combination, it is relatively straightforward to find the atomic single-electron-capture cross sections. Nevertheless these, transmission fractions are still the consequence of entering another additivity "loop," i.e., for σ_{01}.

Since our measurements covered more than two molecules for each (C,X) pairing, these atomic σ_{10} values are overdetermined and a χ^2 fit was performed. A considerable simplification arose in these fits due to the fact that the H-to-C capture cross-section ratio was 1.6% for 0.8-MeV H^+, and considerably lower at the higher projectile energies. This means that a hydrocarbon molecule looks essentially like a collection of C atoms to the H^+ projectile. Since the relative errors for our experimental results, as presented in Table I, are 2%, it should not, in general, be possible to derive reliable H capture cross sections from our data. Instead the H-to-C capture cross-section ratio was fixed at each projectile energy using the experimental results of Ref. 14. The value of a in Eq. (3) was then varied, in a simultaneous fit to all hydrocarbon data at

each projectile energy, to find the minimum χ^2. There was a broad minimum in the χ^2 versus a curve at $a \sim 3$ for all projectile energies,[29] so an average value $\bar{a}=3.3$ was chosen for all future fits to *all* molecules. With a fixed at 3.3 the values of T for H^+ ranged from 0.345 for T(C;48) at 0.8 MeV in the fluorocarbons to 0.970 for T(C;14) in the hydrocarbons at 3.0 MeV. The transmission fractions for each molecule at each energy are presented in Table II.

Once the values of a and σ_{10}(C) were fixed from the hydrocarbon data analysis it was straightforward to calculate the $\sigma_{10}(C_mX_n)$ molecular values at each projectile energy to compare with the oxide and fluoride data in Table I. In Table I calculated molecular σ_{10} values for the hydrocarbons and oxides and fluorides of carbon, using Eqs. (3) and (4) and the parameters obtained from the above fitting procedure, are given next to their respective experimental values. For H^+ the fitted values in all cases lie within the $\pm 6\%$ absolute errors quoted and in most cases lie within the $\pm 2\%$ relative errors. The largest discrepancy, not surprisingly, is for C_4F_8 which has the smallest transmission fraction of any molecule at any projectile energy.

A similar fitting procedure was applied to the 3.2-MeV-He^+ data in Table I. The best χ^2 value occurred at $a=2.5$ rather than 3.3. A possible reason for the discrepancy is that the loss cross sections for He were extrapolated from lower-energy results and inserted into the fitting routine; hence they could easily be 25% too high. This would account for the lower a value. Calculated molecular σ_{10} values for 3.2-MeV He^+ are presented in Table I. For this case only, since there existed no data for He^+ on H_2 in our energy region, σ_{10}(H) was allowed to vary in the search. The $\sigma_{10}(H)/\sigma_{10}(C)$ ratio was 0.012, quite close—although obviously quite inaccurate—to that for H^+ projectiles (0.016) at the same velocity. The calculated transmission fractions for 3.2-MeV He^+ on the various molecules ranged from 0.284 for T(C;48) in the fluorocarbons to 0.896 for T(C;14) in the hydrocarbons. These T values, as well as those for H^+ projectiles, indicate wide departures from strict additivity. T values for 3.2-MeV He^+ are given in Table II also.

D. Comparison of atomic capture cross sections with theory

In Table III the atomic C, O, and F σ_{10} values derived from this fitting procedure are given for H^+ and He^+ projectiles. The atomic S capture cross section was calculated from the SF_6 total electron-capture cross-section results for H^+ at 1.5, 2.0, and 3.0 MeV by using the previously determined F atomic cross sections and T values computed at each energy (based on data of Ref. 14) with $a=3.3$, inserted into Eq. (4). We present our atomic σ_{10} values with H projectiles for C, O, F, Ne, and S in Fig. 1. For comparison with our Ne results, the data of Ref. 13 are also included; although few points are common between the two data sets, the agreement is quite good over the whole range shown in the figure. Also shown in Fig. 1 are the ECPSSR predictions[25,30,31] for K- and $(K+L)$-shell electron capture by protons from C, O, F, and Ne and the L- and $(K+L+M)$-shell predictions for electron capture by protons from S. Overall the absolute theoretical cross sections predicted by ECPSSR theory[24,25] are in quite good agreement with our extracted and true atomic data, as is evident from the column in Table III labeled $\sigma_{expt}/\sigma_{ECPSSR}$. At the lowest energy, where the outer (L) shell contribution is largest, all the experimental C, O, F, and Ne atomic σ_{10} results fall below the ECPSSR values, with the overall discrepancy increasing with target Z, in line with the increasing L-shell contribution. In the case of S the outer (M) shell contributes only about 10% at the lowest energy, and the experimental σ_{10} value agrees quite well with the ECPSSR prediction.

From the prior discussion of the fitting procedure it is clear that the most reliable atomic σ_{10} values are for C. In Fig. 1 the C results lie quite close in general to the ECPSSR predictions. The O σ_{10} results are not quite as reliable as those for C, and the F results are not as reliable as the O results. This trend arises from the relative magnitudes of the C, O, and F cross sections and the trend toward smaller T values (which have larger propagated errors) for the oxides and fluorides. We believe that reasonable values for the atomic σ_{10} errors would be 10% for C, 14% for O, and 20% for the F. The case of S is somewhat different since these cross sections did not arise from a fit, but were unique solutions of Eq. (4) (as explained in

TABLE III. Atomic electron-capture cross sections for C, O, F, Ne, and S with 0.8—3.0-MeV H^+ and 3.2-MeV He^+ compared to ECPSSR predictions. (All cross sections in 10^{-21} cm^2.) C, O, F, and S cross sections derived from molecular targets.

		C[a]		O[b]		F[c]		Ne[d]		S[e]	
	E_p (MeV)	σ_{expt}	σ_{ECPSSR}	σ_{expt}	σ_{ECPSSR}	σ_{expt}	σ_{ECPSSR}	σ_{expt}	σ_{ECPSSR}	σ_{expt}	σ_{ECPSSR}
H^+	0.8	45	0.77	55	0.55	79	0.53	104	0.48		
	1.5	7.8	1.04	8.1	1.04	9.8	1.02	10.7	0.72	35	1.07
	2.0	2.7	0.88	3.1	0.99	3.2	0.92	3.5	0.81	20	1.64
	3.0	0.52	0.79	0.78	0.99	0.84	1.01	0.89	1.01	2.7	1.04
He^+	3.2	165	0.20	169	0.13	266	0.14				

[a]Absolute errors $\pm 10\%$.
[b]Absolute errors $\pm 14\%$.
[c]Absolute errors $\pm 20\%$.
[d]Absolute errors $\pm 6\%$—data from Table I.
[e]Absolute errors $\pm 30\%$.

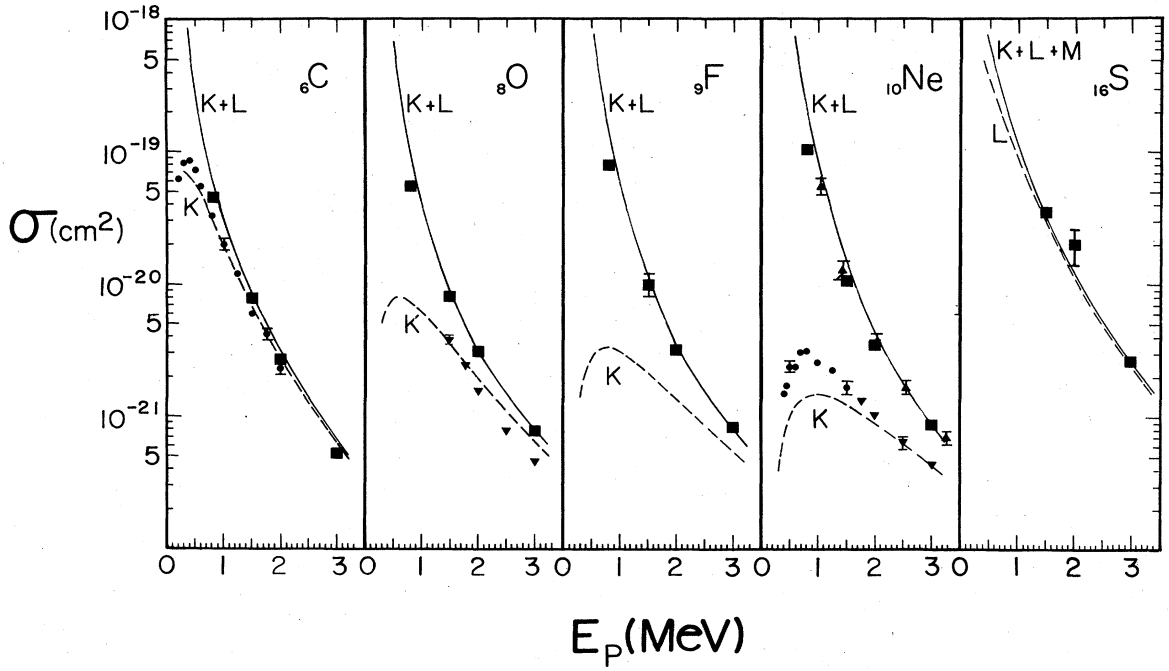

FIG. 1. Atomic total electron-capture cross sections for H^+ on C (derived from hydrocarbon measurements), O (derived from oxide data with C cross sections fixed from hydrocarbon data analysis), F (derived from fluorocarbon data with C cross section fixed from hydrocarbon data analysis), Ne (Table I), and S (derived from SF_6 data with F fixed from fluorocarbon data analysis). Data shown: ■, this work (errors smaller than data points for C and Ne, equal for O and as shown for F and S); ▲, Ref. 13 for Ne total electron-capture cross sections; ●, Ref. 32 for capture from C and Ne K shells; ▼, Ref. 33 for capture from O and Ne K shell. ECPSSR predictions for K (— — —) and $K+L$ (——) shells (C, O, F, Ne) and L (— — —) and $K+L+M$ (——) for S are shown for comparison (Refs. 25 and 30).

TABLE IV. Comparison of experimental and ECPSSR predictions for $(K+L)/K$ electron-capture cross sections for 0.8—3.0-MeV H^+ on C, O, and Ne. (All cross sections in 10^{-21} cm.)

Target	E_p (MeV)	σ_{K+L} (expt.)[a]	σ_K (expt.)[b,c]	σ_{K+L}/σ_K (expt.)[d]	σ_{K+L}/σ_K (ECPSSR)[e]
C	0.8	45 ±4.5	33 ± 2 (0.910)	1.24±0.14	1.89
	1.5	7.8 ±0.8	6.0 ±0.3 (0.945)	1.23±0.14	1.19
	2.0	2.7 ±0.3	2.3 ±0.2 (0.958)	1.12±0.13	1.11
O	1.5	8.1 ±1.1	3.8 ±0.3[f] (0.918)	1.96±0.31	2.38
	2.0	3.1 ±0.4	1.58±0.16 (0.927)	1.82±0.31	1.60
	3.0	0.78±0.11	0.47±0.05 (0.941)	1.56±0.27	1.22
Ne	0.8	104±6	3.20±0.28	32.5 ±3.5	134
	1.5	10.7 ±0.6	1.70±0.20	6.3 ±0.8	11.2
	2.0	3.52±0.21	1.07±0.09	3.27±0.34	4.63
	3.0	0.89±0.05	0.45±0.03	1.98±0.18	1.99

[a]This work—Table I.
[b]References 32 (CH_4) and 33 (O_2).
[c]Number in parentheses below the σ_K values for molecular targets is the relevant transmission fraction from Table II.
[d]Ratio corrected for exit effect.
[e]References 25 and 30.
[f]This data point actually at 1.48 MeV, which will slightly reduce the $(K+L)$- to K-shell electron-capture cross-section ratio.

a prior discussion), using predetermined F cross sections which themselves introduced 20% errors; here reasonable errors would be 30% for S. In terms of these errors the agreement between experiment and theory is quite acceptable for these derived atomic cross sections, and quite similar to that obtained for the case of Ne. The method of deriving atomic electron-capture cross sections from molecular electron-capture cross sections, as outlined above, is applicable in principle to any molecule of any size, with any number of atomic species, if a sufficiently broad range of pertinent capture and loss cross sections is available.

Since there are no actual atomic total σ_{10} measurements available to compare with our extracted atomic cross sections, we can only provide a somewhat weaker test of their reliability by computing the experimental ratio of total $(K+L)$- to K-shell electron-capture cross sections for comparison to theoretical predictions. Theoretical predictions of electron-capture cross sections from the L shell are generally less reliable than those for the K shell. In regions where the L-shell contributions to the total capture cross section are small, however, the theoretical $(K+L)$- to K-shell electron-capture cross-section ratio should be a relatively reliable number. This theoretical ratio can be compared directly to the equivalent experimental ratio by using the recent measurements on electron capture from the C K shell in a CH_4 target by Rødbro, Horsdal-Pedersen, Cocke, and Macdonald,[32] in conjunction with our $K+L$ cross sections (both for H^+ projectiles). Since capture from the K shell of C (or O or F) is expected to be quite insensitive to the chemical bonds (if any) of the outer-shell electrons, these measurements qualify as atomic in the entrance-effect sense. Moreover, the H contribution to the $K+L$ capture cross section for hydrocarbons by $\sim$MeV/u projectiles is quite small, further simplifying matters. It should be noted that measured K-shell capture cross sections are still sensitive to the exit effect since the projectile must pass through the remainder of the CH_4 molecule, hence we have corrected the cross sections of Rødbro *et al.* by using the transmission fractions for capture from the C as listed in Table II for CH_4. In Table IV, experimental $(K+L)$- to K-shell electron-capture cross-section ratios are presented for comparison with the ECPSSR predictions. Similarly, $(K+L)$- to K-shell ratios computed for the O data by using the data of Cocke, Gardner, Curnette, Bratton, and Saylor[33] for K-shell electron-capture cross sections from O_2 are presented in Table IV. We have omitted the data of Ref. 33 for O below 1.5 MeV since they are believed to be inaccurate.[32] As in the C ratios above, the data from Ref. 33 are corrected by the relevant transmission fraction from Table II.

Overall the agreement in experimental and ECPSSR $(K+L)$- to K-shell electron-capture cross-section ratios is quite good. However, when the L shell is the dominant contributor to the total capture cross section, as is the case for Ne at 0.8, 1.5, and 2.0 MeV (using experimental results from this work and Refs. 32 and 33), the agreement is much worse in the $(K+L)$- to K-shell ratio as can be seen in Table IV; at 3.0 MeV the $(K+L)$- to K-shell ratio is within error of the ECPSSR prediction. The data of Refs. 32 and 33 for C, O, and Ne (uncorrected for the exit effect) are also presented in Fig. 1. The good agreement observed between the experimental and ECPSSR $(K+L)$-to K-shell ratios for C, O, and Ne that occurs when the L-shell contribution to the total electron-capture cross section is relatively small tends to buttress the reliability of all the atomic electron-capture cross sections extracted from molecular measurements.

V. CONCLUSIONS

We have measured the total electron-capture cross sections for 0.8—3.0-MeV H^+ and 3.2-MeV He^+ from carbon-, oxygen-, fluorine-, and sulfur-bearing molecular gases, as well as Ne. Our measurements and the associated analysis presented in this work imply strongly that there is an underlying order in additivity failure that should be of interest to physicists as well as chemists. Simple, physically justifiable considerations, drawn directly from measurements on atomic and molecular systems, however unsophisticated the model, clearly anticipate just those effects, with the proper magnitudes and trends, that are measured experimentally. Additivity, instead of being treated as just a nostrum or as a measure of last resort, can result in atomic cross sections derived, for the first time with a physical basis, from molecular cross sections.

In the high part of the energy range of our projectiles, target atoms in molecules appear to behave very much as they would singly; additivity failure is much more obvious at the lower projectile energies. The major effect causing additivity failure in the measured molecular single-electron-capture cross sections is the *intra*molecular electron loss, subsequent to the original capture collision, that occurs when the projectile exits the remainder of the molecule. The significance of these results is to open the way to a relatively effortless extraction of atomic σ_{10} values from molecular measurements, using relatively well-understood collision mechanisms; the close agreement between the extracted cross sections and the ECPSSR predictions supports this technique.

ACKNOWLEDGMENT

We would like to thank Gregory Lapicki for useful discussions and for providing the ECPSSR electron-capture cross sections.

*Deceased.
[1]G. H. Henderson, Proc. R. Soc. London Ser. A **227**, 496 (1922).
[2]H. Bartels, Ann. Phys. (Leipzig) **6**, 957 (1930).
[3]J. R. Oppenheimer, Phys. Rev. **31**, 349 (1928).
[4]H. C. Brinkman and H. A. Kramers, Proc. Acad. Sci. Amsterdam **33**, 1331 (1930).
[5]U. Schiebel, B. L. Doyle, J. R. MacDonald, and L. D. Ellsworth, Phys. Rev. A **16**, 1089 (1977).
[6]C. L. Cocke, R. Dubois, T. J. Gray, and E. Justiniano, IEEE Trans. Nucl. Sci. **NS-28**, 1032 (1981).
[7]R. A. Mapleton, *The Theory of Charge Exchange* (Wiley-Interscience, New York, 1972).
[8]K. Taulbjerg, *Fundamental Processes in Energetic Atomic Collisions,* edited by H. O. Lutz, J. S. Briggs, and H. Kleinpoppen (Plenum, New York, 1983), p. 349.
[9]S. K. Allison, Rev. Mod. Phys. **30**, 1137 (1958).
[10]H. D. Betz, Rev. Mod. Phys. **44**, 465 (1972).
[11]H. Tawara and A. Russek, Rev. Mod. Phys. **45**, 178 (1973).
[12]L. M. Welsh, K. H. Berkner, S. N. Kaplan, and R. V. Pyle, Phys. Rev. **158**, 85 (1967).
[13]U. Schryber, Helv. Phys. Acta **39**, 562 (1966); **40**, 1023 (1967).
[14]L. H. Toburen, M. Y. Nakai, and R. A. Langley, Phys. Rev. **171**, 562 (1966).
[15]S. L. Varghese, G. Bissinger, J. M. Joyce, and R. Laubert, Nucl. Instrum. Methods **170**, 269 (1980).
[16]C. L. Cocke, J. R. MacDonald, B. Curnutte, S. L. Varghese, and R. R. Randall, Phys. Rev. Lett. **36**, 782 (1976).
[17]E. Horsdal-Pederson, F. Folkmann, and N. H. Pederson, J. Phys. B **15**, 739 (1982).
[18]R. A. Mapleton, Phys. Rev. **130**, 1829 (1963).
[19]D. R. Bates and R. A. Mapleton, Proc. Phys. Soc. London **87**, 657 (1966).
[20]V. S. Nikolaev, Zh. Eksp. Teor. Fiz. **51**, 1263 (1966) [Sov. Phys.—JETP **24**, 847 (1967)].
[21]Y. Band, Phys. Rev. Lett. **37**, 634 (1976).
[22]K. Omidvar, Phys. Rev. A **19**, 65 (1979).
[23]W. Fritsch and C. D. Lin, J. Phys. B **16**, 1595 (1983).
[24]G. Lapicki and W. Losonsky, Phys. Rev. A **15**, 896 (1977).
[25]G. Lapicki and F. D. McDaniel, Phys. Rev. A **22**, 1896 (1980).
[26]G. Bissinger, J. M. Joyce, J. Tanis, and S. L. Varghese, Phys. Rev. Lett. **44**, 241 (1980).
[27]G. Bissinger, J. M. Joyce, G. Lapicki, R. Laubert, and S. L. Varghese, Phys. Rev. Lett. **49**, 318 (1982).
[28]G. Bissinger, J. Joyce, R Laubert, and S. L. Varghese, IEEE Trans. Nucl. Sci. **NS-28**, 1149 (1981).
[29]J. M. Joyce and G. Bissinger, IEEE Trans. Nucl. Sci. **NS-30**, 911 (1983).
[30]G. Lapicki (private communication).
[31]Oppenheimer-Brinkman-Kramers σ_{10} cross sections are a factor of 3.00—3.04 higher than ECPSSR predictions over our entire energy range, Ref. 30.
[32]M. Rødbro, E. Horsdal-Pedersen, C. L. Cocke, and J. R. Macdonald, Phys. Rev. A **19**, 1936 (1979).
[33]C. L. Cocke, R. K. Gardner, B. Curnutte, T. Bratton, and T. K. Saylor, Phys. Rev. A **16**, 2248 (1977).